Am J Transl Res 2021;13(4):1990-2005
www.ajtr.org /ISSN:1943-8141/AJTR0103470

Original Article

Substance P-induced RAD16-I scaffold mediated hUCMSCs stereo-culture triggers production of mineralized nodules and collagen-like fibers by promoting osteogenic genes expression

Yuan Li*, Shuyin Zhang*, Wantao Li*, Xueni Zheng, Yang Xue, Kaijin Hu, Hongzhi Zhou

*State Key Laboratory of Military Stomatology, National Clinical Research Center for Oral Diseases, Shaanxi Clinical Research Center for Oral Diseases, Department of Oral and Maxillofacial Surgery, School of Stomatology, The Fourth Military Medical University, Xi'an 710032, PR China. *Equal contributors.*

Received October 12, 2019; Accepted May 5, 2020; Epub April 15, 2021; Published April 30, 2021

Abstract: Tissue engineering has become an important therapeutic method for injuries. This study aimed to generate collagen-like matrix constructed by hUCMSCs combining self-assembled polypeptide and evaluate differentiated capacity, safety and biocompatibility. Human umbilical cord tissues were isolated and used to primarily culture hUCMSCs. hUCMSCs were identified using immunofluorescence and flow cytometry. Adipogenic- and osteogenic-differentiation of hUCMSCs were evaluated using Oil-red O and Alizarin-Red staining. Self-assembling collagen peptide RAD16-I hydrogel and substance P (SP) were prepared and combined together to form RAD16-I/SP complex. Surface morphology and ultrastructures were observed with scanning electron microscopic (SEM). hUCMSCs in simulated collagen-like matrix environment were plane-cultured and stereo-cultured. Cell viability was examined using CCK-8 and fluorescent staining assay. Osteogenic genes were detected with qRT-PCR and western blot assay. HE staining and Masson staining were used to assess production of mineralized nodules and collagen-like fibers, respectively. Collagen-like matrix complex by combining RAD16-I/SP complex with stereo-cultured hUCMSCs was successfully generated. hUCMSCs in collagen-like matrix complex demonstrated adipogenic-differentiation and osteogenic-differentiation potential. SP-induced RAD16-I mediated stereo-culture of hUCMSCs demonstrated higher cell activity and proliferation potential. SP-induced RAD16-I mediated stereo-culture of hUCMSCs promoted osteogenesis-related molecules expression. SP-induced RAD16-I mediated stereo-culture of hUCMSCs promoted production of mineralized nodules and triggered formation of collagen-like fibers. Cell-collagen-like matrix complex injection (RAD16-I/SP/hUCMSCs complex) exhibited better biocompatibility and no cytotoxicity. In conclusion, SP-induced RAD16-I mediated stereo-culture of hUCMSCs remarkably promoted osteogenesis-related gene expression, triggered production of mineralized nodules and formation of collagen-like fibers. This established cell-collagen-like matrix complex (RAD16-I/SP/hUCMSCs) injection exhibited better biocompatibility, without cytotoxicity.

Keywords: Tissue engineering, self-assembled polypeptide, hUCMSCs, biocompatibility, multidirectional differentiation

Introduction

Tissue and organ damage or dysfunction not only seriously affect the life quality of patients, but also cause an increasingly serious economic burden to society [1, 2]. In the recent years, tissue engineering has become an important therapeutic method for the tissue injury [3]. The basic principle of tissue engineering is to inoculate seed cells into scaffolds with certain biological characteristics after *in vitro* culture and expansion [4]. Then, cell-scaffold complex was implanted into the injured tissues and organs, and finally formed to repair and reconstruct the injured tissues. Tissue engineering is mainly restricted by three important factors, including seed cells, scaffold materials and signal factors. The scaffold material can provide a good three-dimensional structure for the adherence and growth of seed cells, and is conducive to the transport and metabolism of nutrients [5, 6]. Therefore,

scaffold material is a key factor in the application of tissue engineering to repair damage [7].

Generally, tissue engineering scaffolds must be non-toxic, safe, biologically explanatory and easy to produce [8, 9]. Self-assembled polypeptide is a kind of biomaterial with good compatibility and high bioactivity [10]. Especially in recent years, with the continuous exploration of researchers, self-assembled polypeptides have become a hot topic in the field of tissue engineering [11, 12]. Self-assembled polypeptides demonstrate plenty of characteristics [13], including ① the polypeptide sequence of self-assembled polypeptide originates from nature, ② polypeptides have no toxic side effects and immune reactions, ③ polypeptides have good biocompatibility and surface activity, ④ polypeptides can be biodegraded, easily accessible or artificially designed. Therefore, self-assembled polypeptides are considered to be suitable scaffolds for wound repair in tissue engineering centers.

The previous studies [14, 15] have shown that self assembling collagen peptide (RAD16-I), as a water-soluble self-assembled collagen peptide, can form hydrogel state and self assemble into *Nano*-network structure. In the process of self-assembly, cells can be embedded in three-dimensional reticular matrix of RAD16-I, and can migrate freely and interact with each other [16]. Therefore, in this study, we chose human umbilical cord mesenchymal stem cells (hUCMSCs) as the seed cells. hUCMSCs have the functions of self-renewal and proliferation, and have strong multidirectional differentiation potential and cell stability [17]. Therefore, hUCMSCs have shown great potential in regenerative medicine and tissue engineering.

Therefore, in this study, the collagen-like matrix constructed by hUCMSCs combining self-assembled polypeptide was studied by cytological assays. At the same time, this study also attempted to explore the feasibility of tissue engineering scaffold materials in the pre-clinical application.

Materials and methods

Collection and acquisition of human umbilical cord tissues

The umbilical cord tissue used in this study was derived from the remaining umbilical cord of healthy pregnant women who underwent caesarean section. The umbilical cord was freely presented by the Obstetric Ward of Xijing Hospital of Air Force Military Medical University, Xi'an, China. The umbilical cord was collected in a reagent bottle containing DMEM high sugar medium (Hyclone, Logan, UT, USA), containing 5% Penicillin-Streptomycin (SolarBio. SciTech. Co. Ltd., Beijing, China) and stored in laboratory by cryo-preservation of a foam box containing crushed ice.

This study has been approved by the Ethical Committee of the Fourth Military Medical University, Xi'an, China. Meanwhile, all of the pregnant women or their families have provided the written formed consents.

Isolation and primary culture of hUCMSCs

The hUCMSCs were isolated and cultured according to the previous study described [18]. The obtained cells were cultured and the passaged 4 generation (P4 generation) cells were collected for the following experiments. Briefly, the isolated cells were cultured in DMEM medium (Hyclone, Logan, UT, USA), containing 10% fetal bovine serum (FBS, Gibco BRL. Co. Ltd., Grand Island, New York, USA) and supplementing with 5% Penicillin-Streptomycin (SolarBio. SciTech. Co. Ltd.). When, the cells were passaged for 4 generations, the P4 cells were collected.

Identification for hUCMSCs

In this research, the isolated hUCMSCs were identified using immunofluorescence assay and flow cytometry assay. For the immunofluorescence assay, which was conducted according to the previous study [19]. In brief, hUCMSCs were fixed using 4% paraformaldehyde (Sigma-Aldrich, St. Louis, Missouri, USA) for 30 min, permeabilized using Triton-X 100 (Sigma-Aldrich) for 5 min and then blocked using 5% bovine serum albumin (BSA, Beyotime Biotech. Shanghai, China). Then, the cells were incubated with rabbit anti-human CD44 monoclonal antibody (Cat. No. ab189524, 1:500, Abcam Biotech., Cambridge, MA, USA) at 4°C overnight and then incubated with goat anti-rabbit Alexa Fluor 555 labeled IgG (ab150078, Abcam Biotech.) at 37°C for 1 h. The nuclei were also stained using DAPI (SolarBio. SciTech. Co. Ltd., Beijing, China). The immunofluorescence images were captured using laser scanning

confocal microscope (Model: FV3000, Olympus, Tokyo, Japan).

For the flow cytometry assay, which was conducted based on description of previous study [17]. Briefly, hUCMSCs were harvested, washed with PBS and labeled using CD29-FITC, CD44-PE, CD73-FITC, CD90-FITC, CD105-PE, CD34-FITC, CD45-PE and CD106-PE antibodies (BD Bioscience, San Jose, CA, USA). Subsequently, the above stained cells were analyzed using Coulter Epics XL flow cytometer (Coulter Corp., Miami, MI, USA).

Induction of hUCMSCs and adipogenic/osteogenic differentiation

The hUCMSCs were seeded in the 6-well plates (Corning-costar, Corning, NY, USA) in the adipogenic-differentiation medium (DMEM containing insulin, FBS, dexamethasone, indometacin, IBMX), all of which were purchased from Sigma-Aldrich. (St. Louis, Missouri, USA) or osteogenic-differentiation medium (DMEM containing dexamethasone, β-glycerophosphate and ascorbic acid) for 2 weeks, based on the protocols of manufacturers. Post the above induction, adipogenic- or osteogenic-potential was assessed using Oil red O staining (SolarBio. SciTech. Co. Ltd., Beijing, China) and Alizarin red staining.

Preparation of self-assembling collagen peptide RAD16-I hydrogel and substance P (SP)

The self-assembling peptide RAD16-I hydrogel was prepared according to the former study described [20], with some modifications. In brief, the self-assembling peptide scaffold was generated by diluting 100 mg RAD16-I power (with molecular weight of 2315 Da. and purity of 98.0%, with peptide sequence of ARG-PRO-LYS-PRO-GLN-GLN-PHE-PHE-GLY-LEU-MET-NH_2, Ahqzsw Bio., Anhui, China) into the 10 ml sterile double steamed water, mixing uniformity and keeping still for 30 min. Then, the generated self-assembling peptide RAD16-I hydrogel at concentration of 10 mg/ml was stored at 4°C for following usage.

Total of 1.416 mg SP solid powder (with molecular weight of 1348 Da. and purity of 95.2%, with peptide sequence of AcN-RADARADARADARADA-CNH_2, Ahqzsw Bio., Anhui, China) was dissolved into 1 ml sterile double-steamed water. The concentration of SP solution was adjusted to 1×10^{-8} M and stored at 4°C for the following usage.

Scanning electron microscopic (SEM) evaluation of scaffold materials with different combining modes

The self-curing calcium phosphate (CPC) paste (Redpont BioTech., Anhui, China) was prepared by mixing proper amount of CPC powder particles and its solidified liquid in mass/volume (m/V) of 3.0 g:1 ml, which was assigned as CPC group. The RAD16-I was coated in a flat dish and assigned as RAD16-I group. The appropriate amount of CPC powder was mixed with 1×10^{-8} M SP solution in the same proportion and assigned as CPC/SP group. The CPC composite paste was mixed with prepared RAD16-I (10 mg/mL) hydrogel in mass volume ratio (m/V) of 3.0 g:1 ml, which was assigned as CPC/RAD16-I group. The mixture of 1×10^{-8} M SP solution and 10 mg/mL RAD16-I gel was mixed according to the volume ratio (1:1) of the precursor and then mixed with the powder in the above proportion to prepare CPC paste, which was assigned as CPC/SP/RAD16-I group. After the pastes were solidified in a 7 mm × 7 mm × 2 mm casting mould, the samples of each group were placed on a glass plate. The vacuum freeze-drying machine was used to treat the CPC paste, at -60°C for 25 h. Then, the surface of the combining models was treated using spraying gold. The surface morphology and ultra-structure of the combining models were observed using the S-4800 Scanning Electron Microscopy (Hitachi Ltd., Tokyo, Japan) at an accelerated voltage of 5.0 kV.

Culture of hUCMSCs in simulated collagen-like matrix environment

The P4 generation of hUCMSCs was digested when the cell fusion reached to 80%. The cells were suspended in 10% sucrose solution (Redpont BioTech., Anhui, China), and the cell concentration was adjusted to 1×10^5 cells/ml. 24-well plates were added to complete culture medium for blank control group. Another 24-well plates were prepared and cultured in complete culture medium containing 1×10^{-8} M SP solution for each hole as SP group. Control group and SP group were both plane-culture group.

Table 1. Primer sequences for the RT-PCR assay

Genes		Sequences	Length (bp)
ALP	Forward	5'-CCTTGAAAAATGCCCTGAAA-3'	191
	Reverse	5'-CTTGGAGAGAGCCACAAAGG-3'	
RUNX-2	Forward	5'-GAGCTACGAAATGCCTCTGC-3'	173
	Reverse	5'-GGACCGTCCACTGTCACTTT-3'	
COL-1	Forward	5'-TGGTCCTCAAGGTTTCCAAG-3'	123
	Reverse	5'-TTACCAGCTTCCCCATCATG-3'	
OCN	Forward	5'-CATGAGGACCCTCTCTCTGC-3'	153
	Reverse	5'-AGGTAGCGCCGGAGTCTATT-3'	
actin	Forward	5'-GCGACCTCACCGACTACCT-3'	136
	Reverse	5'-GCCATCTCGTTCTCGAAGTC-3'	

In the stereoscopic-culture group, a RAD16-I hydrogel with a concentration of 10 mg/ml was firstly added to the 24-well plate. The above RAD16-I hydrogel was cultured and incubated at 37°C and 5% CO_2 incubator for about 24 h, until the gel was completely bonded. The hUCMSCs were transferred to the P4 generation. When its growth and fusion reached to 80%, it was digested using 10% sucrose solution, and the cell concentration was adjusted to 1×10^5 cells/ml. This treatment of RAD16-I hydrogel as above was assigned as RAD16-I group. Another 24-well plate was prepared and cultured in the complete medium containing 1×10^{-8} M SP solution at dosage of 200 ml/well as the RAD16-I/SP group. RAD16-I group and RAD16-I/SP group were stereo-cultured group. The liquid was changed for the first time after 1 day, and then every 2 days. Cell growth was observed by inverted microscope, and photographed and recorded.

Cell counting kit 8 (CCK-8) assay

The cell suspension (100 ml/well) was inoculated into 96-well plates by adjusting cell dosage of 5×10^4 cells/ml. The cells were pre-cultured for 1 day, 2 days, 3 days, 5 days and 7 days in a humid incubator at 37°C and 5% CO_2. Then, the cells were incubated with 10 μl CCK-8 solution (MP Biomedicals, Irvine, CA, USA) for 2 h. The absorbance value (OD) was measured using enzyme linked immuno-analyzer (Model: ELX-800, Bio-Tek Inc., Winooski, VT, USA), at 450 nm wavelength. The numerical values were plotted as cell proliferation curves.

Cell viability assay

Post the culture of 1st, 3rd, 5th and 7th day, the cells in each group were stained with live/dead fluorescent staining. Cell death fluorescent staining reagents were placed at room temperature, gently patted and blended. The Calcein AM solution (Dojindo, Kumamoto, Japan) and EthD-1 solution (Thermo Fisher Scientific, Hudson, NH, USA) were centrifuged for following usage. The staining solution was prepared by mixing Calcein AM and EthD-1 solution according to volume ratio (v/v) of 1:1 and diluted for 200 folds. The staining solution was added to the cell pore and placed in the incubator at 37°C for 5 min. Under the fluorescence microscopy and blue excitation light, the green represented the living cells and red represented the dead cells. Three random visual fields were selected for each well, and five multiple wells were set to measure the number of viable/dead cells in each well, then the cell viability of each group was calculated. The formula for calculating viable cell force was listed as the following: percentage of viable cells = number of viable cells/(number of viable cells + number of dead cells) × 100%.

Quantitative real-time PCR assay (qRT-PCR)

RNAs in hUCMSCs were extracted using TRK cell lysate containing β-mercaptoethanol (Kehao BioTech., Hanzhou, China). Complementary DNAs (cDNAs) were also generated with Reverse Transcription Kit (Cat. No. GA30333, Omega Bio-Tek, Inc., Atlanta, USA) based on manufacturer's protocol. The mRNA expression of ALP, RUNX-2, COL-1, OCN and β-actin was measured with SYBR PrimeScipt Plus RT-PCR Kit (Cat. No. DRR096A, Takara BioTech., Dalina, China) using the Real-time Fluorescence quantitative PCR reactor (Model: ABI-7500, Thermo Fisher Scientific, Waltham, MA, USA). The primers used in this study were listed in **Table 1**. All of the amplified genes were analyzed using professional Gel Scanning System (Model: GDS8000, UVP, Sacramento, CA, USA) due to the equipment's protocol. The final gene expressions were evaluated using method of $2^{-\Delta\Delta ct}$, depending on protocol of the previous document [21].

Western blot assay

Expression of osteogenic molecules, including ALP, RUNX-2, COL-1, OCN, were also examined with western blot assay. The hUCMSCs cells

were lysed with Trizol lysate (Beyotime Biotech.) for 10 min and centrifuged at 10000 r/min to harvest protein. Protein's concentration was determined with BCA protein assay kit (Beyotime Biotech). The obtained proteins were loaded onto SDS-PAGE gel and electrotransferred onto PVDF membrane (AB, Piscataway, NJ, USA). Then, the PVDF membranes were treated with mouse anti-human OCN antibody (Cat. No. ab13418, Abcam, Cambridge, Massachusetts, USA), rabbit anti-human ALP antibody (Cat. No. ab83259, Abcam), rabbit anbti-human RUNX-2 antibody (Cat. No. 860-139, ZEN Bio., Chengdu, China), rabbit anti-human COL-1 antibody (Cat. No. 14695-1-AP, Proteintech, Rosemont, IL, USA) and rabbit anti-human GAPDH antibody (Cat. No. ab181-602, Abcam) at 4°C overnight. Then, PVDF membranes were also treating using HRP-labeled goat anti-rabbit IgG (Cat. No. 12-348, Sigma-Aldrich, St. Louis, Missouri, USA) or HRP-labeled goat anti-mouse IgG (Cat. No. 12-349, Sigma-Aldrich) at room temperature for 2 h. Western blot bands were imaged with ECL imaging kit (Beyotime Biotech.) and images were analyzed using Labworks Analysis Software (Bio-Rad., Hercules, CA, USA). Relative protein expression of ALP, RUNX-2, COL-1, OCN was represented as ratio of western blot band grey density normalized to grey density of GAPDH protein.

Histological staining

HE staining: After 4 weeks of incubation, the cells were washed using PBS and fixed with 4% PFA for 15 min. Then, cells were paraffin-embedded and cut into sections with thickness of 5 μm. Post the dewaxing, the dewaxed ethanol gradient was conducted to dehydrate the water from sections, which were then incubated with hematoxylin (Beyotime Biotech., Shanghai, China) for 15 min. Post washing with ddH_2O, the sections were removed into the differentiating solution and incubated for 10 min, flowing with washing for 30 min and staining with eosin (Beyotime Biotech.) for 5 min. The cells were dried after washing with running water and sealed with neutral gum. The morphology and differentiation of cells were observed under a microscope (Model: CX22, Olympus, Tokyo, Japan) and photographed.

Masson staining: The paraffin embedded sections were dewaxed and washed using distilled water. Then, the sections were nucleated with Weigert hematoxylin (Beyotime Biotech.) for 5 s, stained with Masson Lichunhong acid reddish solution (Beyotime Biotech.) for 10 min, differentiated with 1% phosphomolybdic acid solution (Sigma-Aldrich) for 5 min, and dyed with aniline blue (Sigma-Aldrich) for 5 min. Subsequently, the sections were washed with 0.2% glacial acetic acid solution (Sigma-Aldrich) for 5 s. Post the dehydration of 95% alcohol and anhydrous alcohol (Beyotime Biotech.), transparent with xylene (Fuyu Chem. Industry, Shandong, China) and sealed with neutral gum, the results were observed and analyzed under the microscope (Model: CX22, Olympus, Tokyo, Japan).

Cell viability measurement of cell-collagen-like matrix complex

The feasibility of injecting the cell-collagen-like matrix complex (RAD16-I or RAD16-I/SP) in Stereo-culture group was studied. The cells in the culture plates were sucked up by syringe and then injected back into the culture plates. The cell viability was measured post the 24 h of incubation.

Scanning electron microscopic observation for osteoid-matrix environment simulated cell-scaffold complex

CPC was injected into the cell-collagen-like matrix complex with a double-barrel syringe. After it was completely solidified, CPC was placed in a freeze-dryer for 25 h. The ultrastructure and cell morphology of the material-cell complex were observed under Scanning Electron Microscopy (Hitachi Ltd., Tokyo, Japan).

Statistical analysis

The SPSS17.0 software (IBM SPSS, Inc., Chicago, IL, USA) was utilized for the statistical analysis. Student's t test was applied to compare values between two independent variables. In the case of homogeneity of variance, the ANOVA was applied to compare values of multiple samples, while the Kruskal-Wallis rank sum test was applied in case of variance heterogeneity. The multiple comparisons between two groups were analyzed using the least significant difference *t* (LSD-t). When the *p* value less than 0.05, it was considered as the statistically significant.

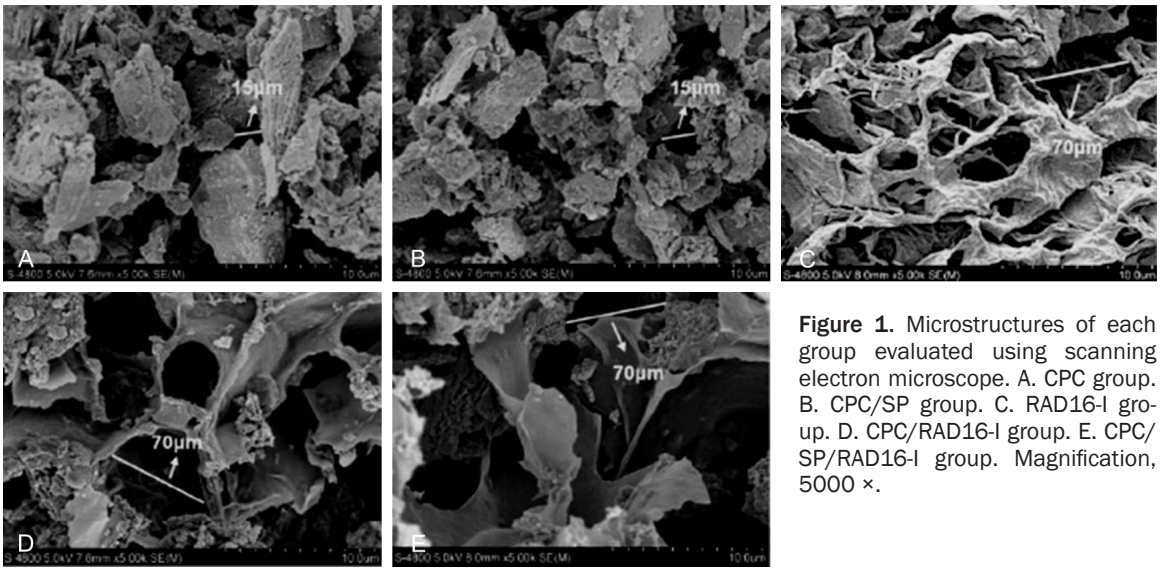

Figure 1. Microstructures of each group evaluated using scanning electron microscope. A. CPC group. B. CPC/SP group. C. RAD16-I group. D. CPC/RAD16-I group. E. CPC/SP/RAD16-I group. Magnification, 5000 ×.

Results

SEM findings for scaffold materials with different combining modes

SEM findings showed that on surface of scaffold materials in single CPC group (**Figure 1A**) and CPC/SP group (**Figure 1B**), the CPC was irregular and closely arranged with different particle diameters. Meanwhile, the pore diameter between particles was about 10 microns. In RAD16-I group (**Figure 1C**), post freeze-drying, the surface was smooth, showing a sponge-like three-dimensional mesh porous collagen-like structure. And the pore diameter was about 50-70 microns. The results of CPC/RAD16-I (**Figure 1D**) and CPC/SP/RAD16-I (**Figure 1E**) demonstrated that the pore size between CPC and RAD16-I increased to 70 micron post the mixture of RAD16-I and CPC was lyophilized.

Morphological evaluation and identification of hUCMSCs

The umbilical cord tissues were isolated and digested using type I collagenase to obtain the primary hUCMSCs (**Figure 2A**). The hUCMSCs were primarily passaged from P1 to P3 generation and observed under the inverted microscope. The cells were gradually extended from round to long spindle shape with close adherence arrangement, and fused for about 5-7 days (**Figure 2B**). Cell growth curve was drawn according to the number of primary cells and sub-cultured cells. The results indicated that hUCMSCs amounts of P1, P2 and P3, were increased following with the prolonged culturing time (from day 1 to day 7) (**Figure 2C**).

The immunofluorescence assay results showed that the specific marker CD44 was positively expressed in hUCMSCs, and nucleus of cells stained with DAPI showed blue fluorescence (**Figure 2D**). The purity of hUCMSCs was over 90% due to the immunofluorescence identification. Moreover, the flow cytometry findings exhibited that the expression rates stem cell surface biomarkers, including CD29, CD44, CD73, CD90 and CD105 were 96.4%, 95.2%, 84.7%, 92.7% and 98%, respectively. Meanwhile, expression rates of hematopoietic biomarkers, including CD34, CD45 and CD106 were 1.9%, 2.9% and 4%, respectively (**Figure 2E**). Therefore, the cultured cells were identified as hUCMSCs.

hUCMSCs demonstrated multidirectional differentiation potential

The adipogenic induction Oil red O staining results indicated that hUCMSCs demonstrated no lipid droplets in Control group, while demonstrated the red-stained lipid droplets staining in Induction group (**Figure 3A**). The osteogenic induction Alizarin red staining results showed that hUCMSCs demonstrated obvious reddish-brown mineralized nodules in Induction group and without obvious mineralized nodules in Control group (**Figure 3B**).

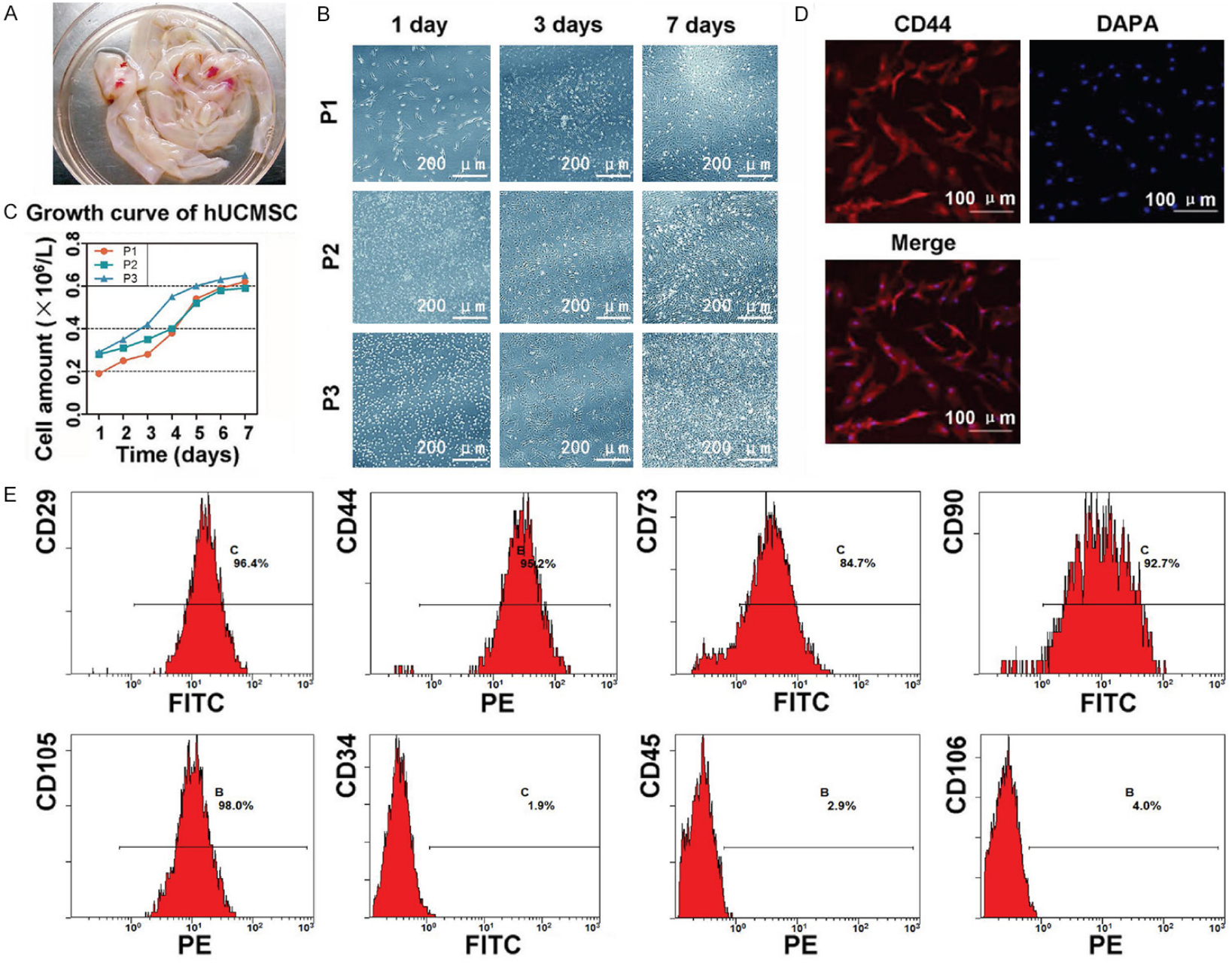
A
B
1 day
3 days
7 days
P1
P2
P3
200 μm
C Growth curve of hUCMSC
Cell amount (×10⁶/L)
Time (days)
P1
P2
P3
D
CD44
DAPA
Merge
100 μm
E
CD29
C 96.4%
CD44
B 95.2%
CD73
C 84.7%
CD90
C 92.7%
CD105
B 98.0%
CD34
C 1.9%
CD45
B 2.9%
CD106
B 4.0%
FITC
PE

Figure 2. Isolation, primary culture and identification of hUCMSCs. A. Isolated human umbilical cord tissues. B. Morphological observation of cells from P1 to P3 under inverted microscope (scale bar =200 μm). C. Growth curve of hUCMSCs from P1 to P3. D. Immunofluorescence detection for hUCMSCs (scale bar =100 μm). E. Flow cytometry detection of specific markers of hUCMSCs.

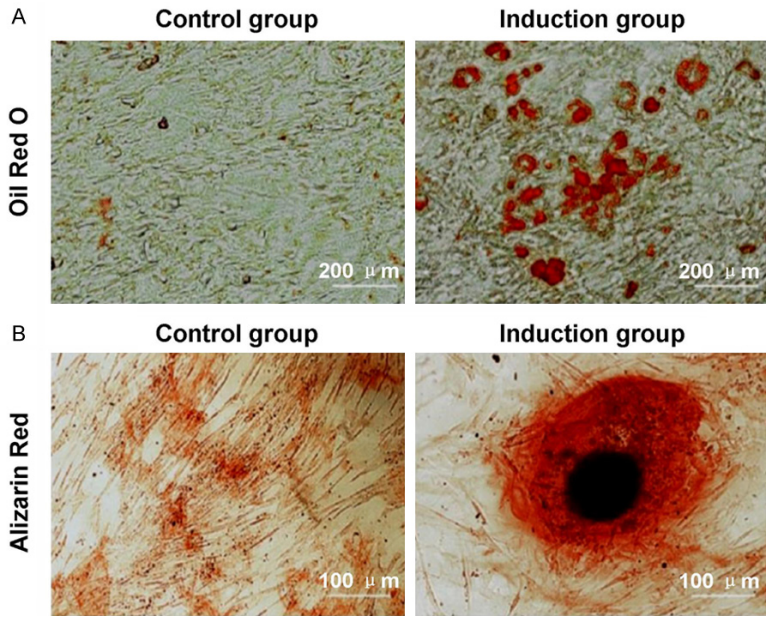

Figure 3. Evaluation for adipogenic-differentiation and osteogenic-differentiation of hUCMSCs under inverted microscope. A. Adipogenic-differentiation of hUCMSCs using Oil red O staining. B. Osteogenic-differentiation of hUCMSCs using Alizarin red staining. Scale bar =200 μm.

Growth of hUCMSCs under plane-culture and stereoscopic-culture

Cell growth and morphological structure of plane cell culture group and three-dimensional cell culture group were observed using microscope. The results showed that the cells in plane-culture groups (Control group (**Figure 4A**) and SP group (**Figure 4B**)) and stereoscopic-culture groups (RAD16-I (**Figure 4C**) and RAD16-I/SP group (**Figure 4D**)) grew well. Meanwhile, the plane-culture group (2D group) illustrated no obvious cell colony (**Figure 4E**), and hUCMSCs in stereoscopic-culture group (3D group) were clustered and gradually extended (**Figure 4F**).

CCK-8 results showed that the cell proliferation rate of Control group was the lowest among all time points, compared with the other 3 groups (**Figure 4G**). At the same time, the cell growth in each group increased logarithmically from 3rd days to 5th days, while, the proliferation activity of the remaining three groups was significantly higher compared to that of the Control group on the 7th day (**Figure 4G**, $P<0.05$). However, there was no significant statistical difference among SP group, RAD16-I group and SP/RAD16-I group (**Figure 4G**, $P>0.05$).

SP-induced RAD16-I mediated stereo-culture of hUCMSCs demonstrated higher cell activity and proliferation potential

Calcein AM/EthD-1 staining of living/dead cells findings showed that most cells in different culture environments and conditions showed green fluorescence staining, and the number of cells increased gradually with the prolonged time (**Figure 5A**). At the same time, cell morphology gradually extended, showing long spindle or irregular polygon, and a few cells were red stained without significant difference between groups (**Figure 5B**, $P>0.05$). Cells in each group maintained a high degree of stability, and there was no significant difference in cell activity and proliferation potential among the components (**Figure 5B**, $P>0.05$).

SP-induced RAD16-I mediated stereo-culture of hUCMSCs promoted osteogenesis-related molecules expression

After culturing for 4 weeks in different culture environments, expression of osteogenesis-related genes, including OCN (**Figure 6A**), RUNX-2 (**Figure 6B**), ALP (**Figure 6C**) and COL-1 (**Figure 6D**), was evaluated using RT-PCR assay. The data showed that expression of osteogenesis-related genes in 1×10^{-8} M SP-induced plane-culture group and self-assembling collagen peptide RAD16-I structured stereo-culture group was remarkably higher compared to that in Control group (**Figure 6**, $P<0.05$). Meanwhile, expressions of OCN, RUNX-2, ALP and COL-1

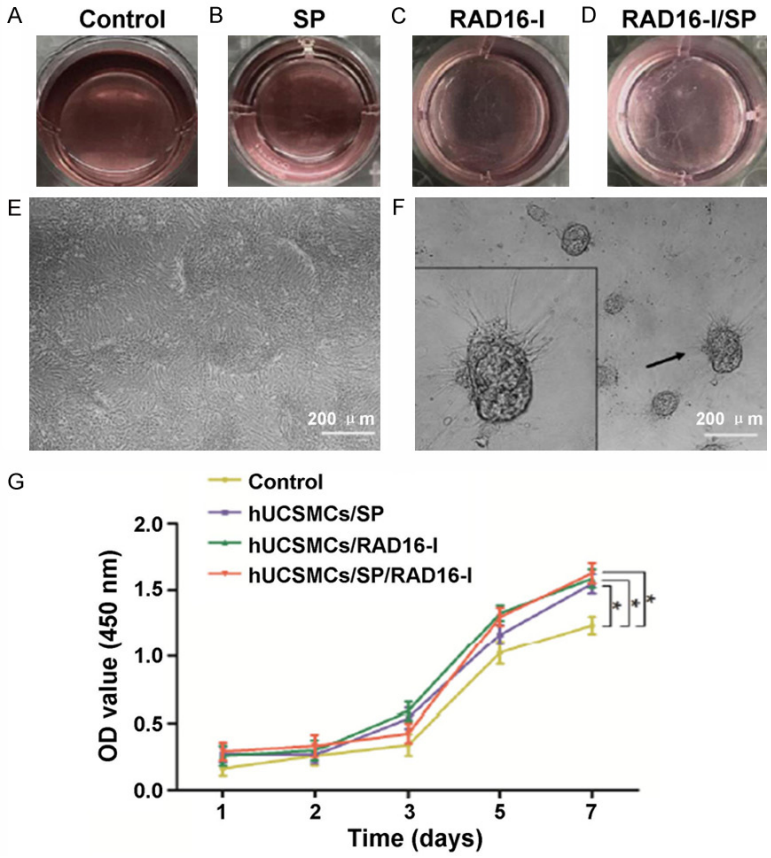

Figure 4. Growth and proliferation of both stereo-cultured and plane-cultured hUCMSCs. A. hUCMSCs growth of Control group within 1 week of culture. B. hUCMSCs growth of SP group within 1 week of culture. C. hUCMSCs growth of RAD16-I group within 1 week of culture. D. hUCMSCs growth of RAD16-I/SP group within 1 week of culture. E. Plane-cultured (2D cultrue) group observed under an inverted microscope (scale bar =200 μm). F. Stereo-cultured (3D culture) group observed under an inverted microscope. The arrow showed the cell mass (scale bar =200 μm). G. Comparison of cell proliferation between different groups in different culture environments. *P<0.05 represented the differences between the illustrated two groups.

genes in SP-induced plane-culture group were significantly higher compared to those in plane-culture group without SP induction (**Figure 6**, P<0.01). For expression of RUNX-2 gene, 1 × 10^{-8} M SP-induced RAD16-I stereo-culture group was remarkably higher compared to that in SP-induced RAD16-I plane-culture group (**Figure 6**, P<0.05). There was no significant difference in gene expression between RAD16-I stereo-culture group and Control group (**Figure 6**, P>0.05). Therefore, different culture environments and conditions could obviously influence the expression of osteogenesis-related genes.

Moreover, the western blot assay was also conducted to clarify the effects of SP-induced RAD16-I mediated stereo-culture of hUCMSCs on osteogenesis-related molecules expression (**Figure 7A**). The western blot assay results consisting with the PCR assay findings that SP-induced RAD16-I mediated stereo-culture of hUCMSCs significantly promoted the OCN (**Figure 7B**), COL-1 (**Figure 7C**), ALP (**Figure 7D**) and RUNX-2 (**Figure 7E**) protein expression compared to the other groups (P<0.05).

SP-induced RAD16-I mediated stereo-culture of hUCMSCs promoted production of mineralized nodules

The hUCMSCs were cultured in different culture environments for 4 weeks and then stained with Alizarin red method. The results illustrated that obvious reddish brown mineralized nodules were observed in both plane-culture group and stereo-culture group (**Figure 8A**). However, amounts of calcium nodules were remarkably increased in 1 × 10^{-8} M SP-induced RAD16-I stereo-culture group and SP-induced plane-culture group (**Figure 8A**). Meanwhile, no mineralized nodules were discovered in Control group (**Figure 8A**).

SP-induced RAD16-I mediated stereo-culture of hUCMSCs triggered formation of collagen-like fibers

The hUCMSCs were cultured in different culture environments for 4 weeks and then stained with HE staining and Mason staining method. HE staining results demonstrated that hUCMSCs in 1 × 10^{-8} M SP-induced plane-culture group were clustered and closely connected with each other (**Figure 8B**). Meanwhile, comparing with Control group, the surface area of cell clusters significantly increased and the staining significantly deepened (**Figure 8B**). In the stereo-culture group, part of RAD16-I was red stained, which was the same as that of the simulated extra-cellular matrix (**Figure 8B**). The

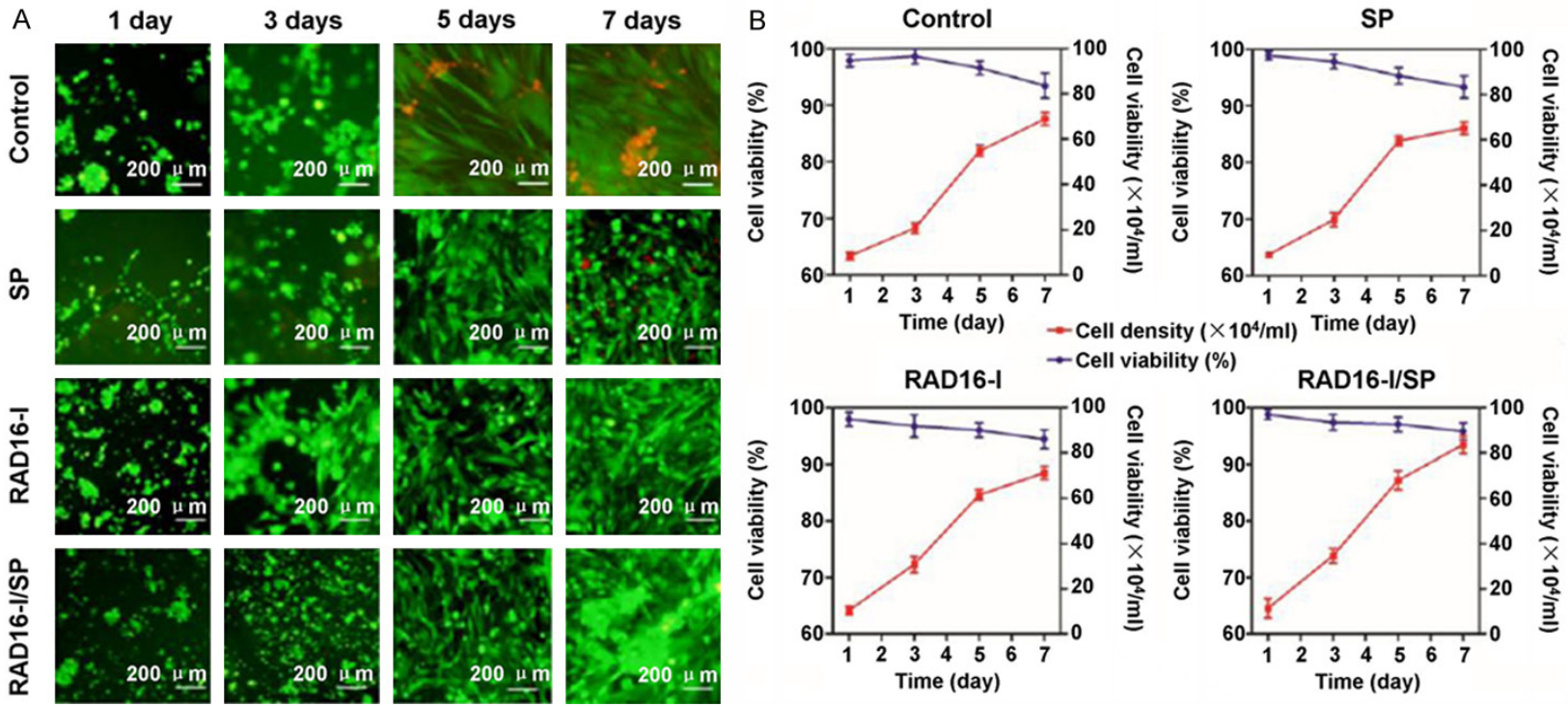

Figure 5. Determination for the live/dead cell staining using fluorescence assay. A. Fluorescence staining of live/dead cells. B. Statistical analysis for cell viability and growth curve in each group (scale bar =200 μm).

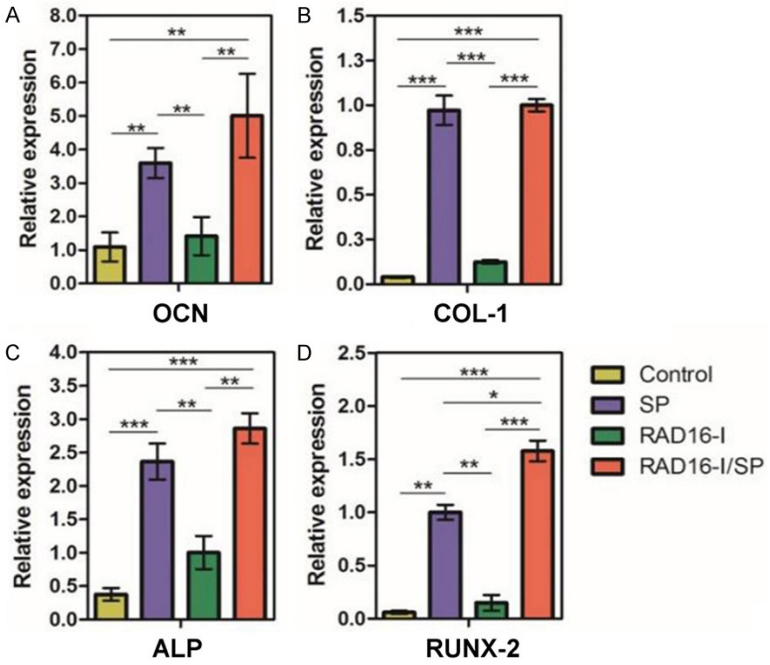

Figure 6. Examination for osteogenesis-related genes expression in 4 weeks cultured hUCMSCs of each group using RT-PCR assay. A. Statistical for OCN mRNA expression. B. Statistical for COL-1 mRNA expression. C. Statistical for ALP mRNA expression. D. Statistical for RUNX-2 mRNA expression. $^{*}P<0.05$, $^{**}P<0.01$, $^{***}P<0.001$ represented the differences between the illustrated two groups.

structure of collagen-like fibers was light pink, and the cytoplasm and surrounding areas were bright red with strong reflections. However, in the 1 × 10^{-8} M SP-induced RAD16-I stereo-culture group, a small amounts of bone matrix-like blue staining began to appear around the hUCMSCs post 4 weeks culture (**Figure 8B**).

Masson staining findings exhibited that the SP group demonstrated obviously higher cell aggregation and deeper staining compared to that of Control group (**Figure 8C**). The collagen-like fibers were blue-stained in matrix around the RAD16-I cells in 1 × 10^{-8} M SP-induced RAD16-I stereo-culture group (**Figure 8C**). More importantly, the density of blue-stained collagen-like fibers in 1 × 10^{-8} M SP-induced RAD16-I stereo-culture group was remarkably higher compared to that of SP-induced RAD16-I stereo-culture group (**Figure 8C**).

Cell-collagen-like matrix complex injection exhibited no cytotoxicity

The cytotoxicity of cell-collagen-like matrix complex (RAD16-I or RAD16-I/SP) injected hUCMSCs was evaluated using live/dead fluorescent staining. The results illustrated that the fluorescent staining of cells in each group before and after injection was green, most of them were living cells, and the cells were clustered and stretched in lumps (**Figure 9A**). The statistical analysis findings showed that there was no significant difference for the cell viability between Control group and Injection group for both of RAD16-I or RAD16-I/SP cell-collagen-like complex (**Figure 9B**, $P>0.05$).

Osteoid-matrix environment simulated hUCMSCs-scaffold (SP-induced RAD16-I) complex exhibited better biocompatibility

SEM data showed that post the freeze-drying of CPC/RAD16-I/hUCMSCs complex, the hUCMSCs expanded orderly and tightly bound to the composites (**Figure 10**). The cells grew in a long spindle shape and had good biocompatibility.

Discussion

In field of tissue engineering, self-assembling technology of collagen-like polypeptide molecules has been become a research hot-spot in constructing new small biological molecular carriers [22, 23]. Self-assembled collagen-like polypeptide molecules have special sequences, polar and non-polar surfaces and special structures of amino acid complementary bands. In recent years, self-assembled collagen-like polypeptides have shown some significant advantages [24, 25], including favorable to cell attachment and growth, higher specificity and biological activity, huge surface-area allowing attachment of specific bioactive and nutrient factors and demonstration of less immunogenicity/pathogenicity, without any cytotoxicity and side-effects.

Mesenchymal stem cells need to be expanded and cultured *in vitro* to obtain enough cells

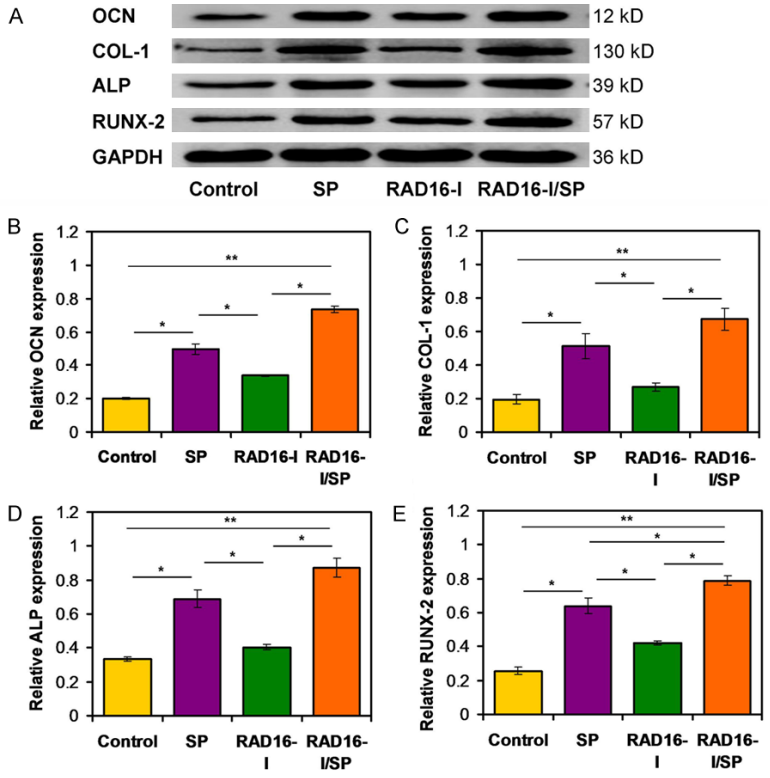

Figure 7. Determination for the osteogenesis-related molecules expression in 4 weeks cultured hUCMSCs of each group with western blot assay. A. Western Blot of OCN, COL-1, ALP and RUNX-2 protein expression. B. Statistical analysis of the OCN gene expression. C. Statistical analysis of the COL-1 gene expression. D. Statistical analysis of the ALP gene expression. E. Statistical analysis of the RUNX-2 gene expression. $^{*}P<0.05$ and $^{**}P<0.01$ represented differences between the illustrated two groups.

before they can be used in basic and clinical research and treatment [26, 27]. Presently, *in vitro* cell expansion and culture is mainly plane-culture (2D culture), but most normal human physiological cells grow in stereo-form (3D culture) and play normal physiological functions [28]. Therefore, plane-culture might result in decrease or loss of biological activity of mesenchymal stem cells, leading to premature aging of cells. In this study, in order to maintain biological characteristics of hUCMSCs, we applied RAD16-I collagen peptide gel materials for 3D stereo-culture. However, there is even no study [29] focusing on 3D stereoscopic hUCMSCs cell culture based on self assembling collagen peptide hydrogel RAD16-I. Therefore, this study chose hUCMSCs as seed cells, selected the RAD16-I self-loaded polypeptide as three-dimensional scaffold to carry out the experiments. This study would provide a basis for future stereo-culture of mesenchymal stem cells in transplantation therapy.

The tissue source of hUCMSCs mainly derives from the *Wharton's jelly* and subendothelial layer of umbilical vein [30, 31]. In this study, hUCMSCs were successfully obtained by enzymatic digesting the umbilical cord tissues. The findings showed that the cell growth was stable, proliferation rate was high, and the adherence could be completed within a relatively short time. Microscopic measurement also showed that cell morphology of hUCMSCs in logarithmic phase was long spindle, and the degree of fusion could reach 90% at 9th days of cell growth, with closely polarized cells.

Nowadays, the specific antigen biomarkers of hUCMSCs are not clear, therefore, identification of which mainly conducted using cell morphology analysis, flow cytometry assay and multi-directional differentiation ability method [32]. In our study, the CD44-stained immunofluorescence assay showed that the purity of hUCMSCs even achieved over 90%. The previous literatures [33, 34] also reported that the stem cell surface antigens mainly include CD29, CD44, CD59, CD73 molecules, while hematopoietic cells markers mainly include CD34, CD45, CD106, CD117 molecules. The flow cytometry findings also demonstrated that the surface markers, including CD29, CD44, CD73, CD90 and CD105 of P4 hUCMSCs, were positively expressed while hematopoietic markers, including CD34, CD45 and CD106, were negatively expressed. These results suggest that the cells don't originate from the hematopoietic cells. Therefore, the cells were identified as hUCMSCs. The adipogenic induction Oil red O staining showed the red-stained lipid droplets staining and osteogenic induction Alizarin red staining showed the reddish-brown mineralized nodules in induced hUCMSCs. These resu-

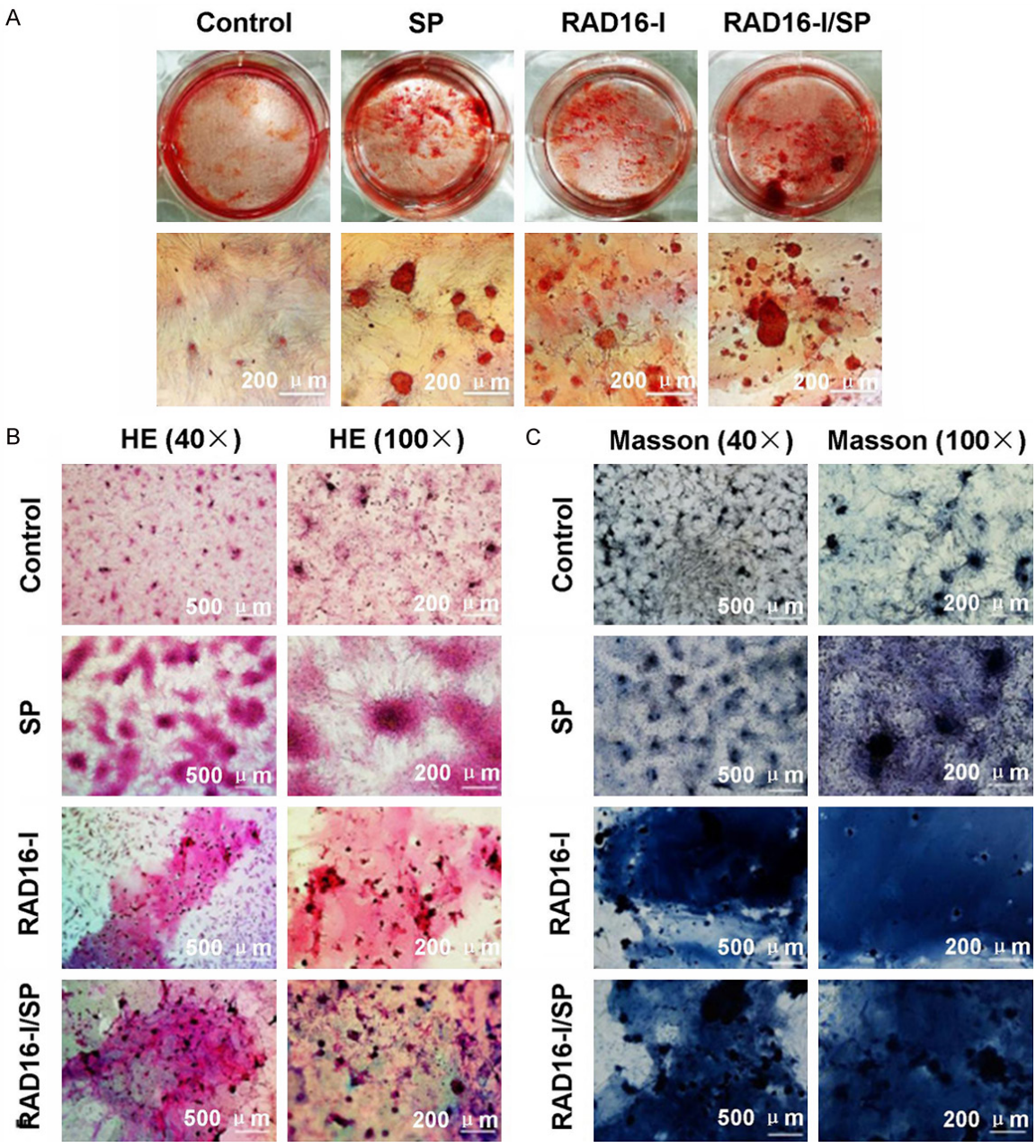

Figure 8. Effects of SP and/or RAD16-I mediated hUCMSCs plane-culture and stereo-culture for 4 weeks on production of mineralized nodules and formation of collagen-like fibers. A. Determination for production of mineralized nodules using Alizarin red staining (scale bar =200 μm). B. Determination for formation of collagen-like fibers using HE staining (40 ×, scale bar =500 μm. 100 ×, scale bar =200 μm). C. Determination for production of collagen-like fibers using Masson staining (40 ×, scale bar =500 μm. 100 ×, scale bar =200 μm).

Its hint that the hUCMSCs demonstrate multidirectional differentiation potential, which is consistent with the previously published documents [35, 36].

In this study, the results of stereo-culture (3D culture) also showed that cells in RAD16-I/SP scaffolds could grow, adhere and proliferate in a short time, as well as aggregated and extended in mass. With the passage of time, the cell mass gradually increased, showing long spindle or irregular polygon. SEM findings showed that the self-assembled collagen-like polypeptide RAD16-I was composed of a large number of nano-fibers with three-dimensional reticular structure, which was conducive to cell

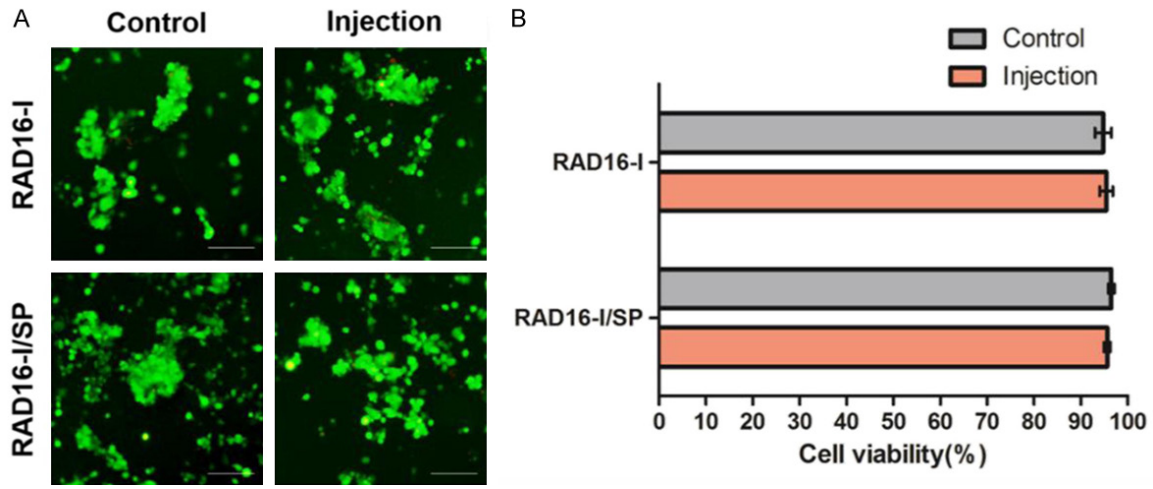

Figure 9. Cytotoxic effects of RAD16-I and RAD16-I/SP injections on hUCMSCs. A. Fluorescence staining of live/dead cells (scale bar =200 μm). B. Statistical analysis for hUCMSCs viability before and post the injection.

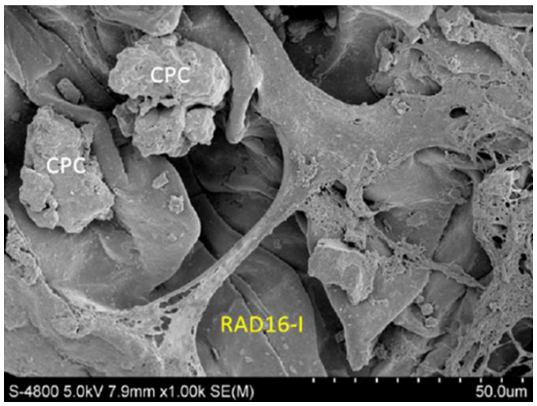

Figure 10. Microstructure of cell-material composites observed under scanning electron microscope (Magnification, 1000 ×).

adhesion and growth. Fluorescence staining of living/dead cells on day 1, day 3, day 5 and day 7 showed that most of cells in RAD16-I group, SP group and RAD16-I/SP group showed green staining, and the number of cells gradually increased. Only a small number of cells in SP group were red stained, and the proportion of living cells was always above 90%. The expressions of OCN, RUNX-2, ALP and COL-1 genes [37] in SP-induced cell plane-culture group and stereo-culture group were significantly higher than those in non-SP-induced plane-culture group and non-SP-induced stereo-culture group. This result fully demonstrates that SP plays an important role in inducing and mobilizing mesenchymal stem cells in process of osteogenic differentiation and expression. At the same time, RAD16-I also provides a stable microenvironment for the release of SP active factors.

The HE staining results showed that the hUCMSCs in SP group were clustered and closely connected with each other, and the surface area of cell clusters was larger and deeper than that in Control group. In stereo-culture group, RAD16-I was red, the structure of collagen-like fibers was light pink, and the cytoplasm and it's surrounding were bright red with strong reflections. Especially in RAD16-I/SP group, a small amount of bone matrix-like blue staining began to appear around hUCMSCs. Masson staining also indicated that SP group demonstrated higher cell aggregation and deeper staining than Control group. Meanwhile, collagen-like fibers were blue stained in surrounding matrix of RAD16-I/hUCMSCs in three-dimensional culture group. The hUCMSCs density of RAD16-I/SP group was remarkably higher compared to that of RAD16-I group. These results indicate that the collagen like peptide molecules could completely simulate extra-cellular matrix components in hydrogel state, and demonstrated good biocompatibility [38]. The hUCMSCs stereo-culture induced by SP mobilization exhibits the tendency of osteogenic transformation. The feasibility of injecting the cell-collagen-like matrix complex in stereo-culture group proved that the material-cell complex was injectable, and the number of living cells in injected complex was more than 90%. In this study, CPC composite solidified freeze-dried cells could adhere to RAD16-I

composites tightly and could also construct composite materials to simulate the morphology and structure of cancellous bone. This laid a foundation for the next step of material injection in animal experiments.

In conclusion, the present study successfully established a kind of collagen-like matrix complex by combining self-assembling collagen peptide RAD16-I/SP complex with stereo-cultured hUCMSCs. SP-induced RAD16-I mediated stereo-culture of hUCMSCs promoted osteogenesis-related gene expression and triggered production of mineralized nodules and formation of collagen-like fibers. The cell-collagen-like matrix complex (RAD16-I/SP/hUCMSCs) injection exhibited no cytotoxicity and exhibited better biocompatibility.

Acknowledgements

This study was granted by National Natural Science Foundation of China (Grant NO. 81371119).

Disclosure of conflict of interest

None.

Address correspondence to: Dr. Hongzhi Zhou, State Key Laboratory of Military Stomatology, National Clinical Research Center for Oral Diseases, Shaanxi Clinical Research Center for Oral Diseases, Department of Oral and Maxillofacial Surgery, School of Stomatology, The Fourth Military Medical University, 145 Western Changle Road, Xi'an 710032, PR China. Tel: +86-029-84776102; Fax: +86-029-84776026; E-mail: hzzhou@fmmu.edu.cn

References

[1] Gefen A, Farid KJ and Shaywitz I. A review of deep tissue injury development, detection and prevention: shear savvy. Ostomy Wound Manage 2013; 59: 26-35.

[2] Souza JD and Gottfried C. Muscle injury: review of experimental models. J Electromyogr Kinesiol 2013; 23: 1253-1260.

[3] Ko SF, Chen YT, Wallace CG, Chen KH, Sung PH, Cheng BC, Huang TH, Chen YL, Li YC, Chang HW, Lee MS, Yang CC and Yip HK. Inducible pluripotent stem cell-derived mesenchymal stem cell therapy effectively protected kidney from acute ischemia-reperfusion injury. Am J Transl Res 2018; 10: 3053-3067.

[4] Yan B, Wei K, Hou L, Dai T, Gu Y, Qiu X, Chen J, Feng Y, Cheng H, Yu Z, Zhang Y, Zhang H and Li D. Receptor-interacting protein 3/caspase-8 may regulate inflammatory response and promote tissue regeneration in the periodontal microenvironment. Med Sci Monit 2018; 24: 5247-5257.

[5] Nune KC, Misra RD, Gaytan SM and Murr LE. Interplay between cellular activity and three-dimensional scaffold cell constructs with different foam structure processed by electron beam melting. J Biomed Mater Res A 2015; 103: 1677-1692.

[6] Sun MH, Wang WJ, Li Q, Yuan T and Weng WJ. Autologous oxygen release nano bionic scafford composite miR-106a induced BMSCs enhances osteoblast conversion and promotes bone repair through regulating BMP-2. Eur Rev Med Phamracol Sci 2018; 22: 7148-7155.

[7] Caccedda R, Giannoni P and Mastrogiacomo M. A tissue engineering approach to bone repair in large animal models and in clinical practice. Biomaterials 2007; 28: 4240-4250.

[8] Baudequin T and Tabrizian M. Multilineage constructs for scafford-based tissue enginnering: a review of tissue-specific challenges. Adv Healthc Mater 2018; 7: 201700734.

[9] Man Z, Li T, Zhang L, Yuan L, Wu C, Li P, Sun S and Li W. E7 pepitide-functionalized Ti6Al4V alloy for BMSC enrichment in bone tissue engineering. Am J Transl Res 2018; 10: 2480-2490.

[10] Zashikhina NN, Volokitina MV, Korzhikov-Vlakh VA, Tarasenko II, Lavrentieva A, Scheper T, Ruhl E, Orlova RV, Tennikova TB and Korzhikova-Vlakh EG. Self-assembled polypeptide nanoparticles for intracellular irinotecan delivery. Eur J Pharm Sci 2017; 109: 1-12.

[11] Li LL, Qi GB, Yu F, Liu SJ and Wang H. An adaptive biointerface from self-assembled functional peptides for tissue engineering. Adv Mater 2015; 27: 3181-3188.

[12] Loo Y, Goktas M, Tekinay AB, Guler MO, Hauser CA and Mitraki A. Self-assembled proteins and peptides as scaffolds for tissue regeneration. Adv Healthc Mater 2015; 4: 2557-2586.

[13] Eskandari S, Guerin T, Toth I and Stephenson RJ. Recent advances in self-assembled peptides: implications for targeted drug delivery and vaccine engineering. Adv Drug Deliv Rev 2017; 110-111: 169-187.

[14] Aloy-Reverte C, Moreno-Amador JL, Nacher M, Montanya E and Semino CE. Use of RGD-functionalized sandwich cultures to promote redifferentiation of human pancreatic beta cells after in vitro expansion. Tissue Eng Part A 2018; 24: 394-406.

[15] Castells-Sala C, Recha-Sancho L, Liucia-Vallderperas A, Soler-Botija C, Bayes-Genis A and Semino CE. Three-dimensional cultures of human subcutaneous adipose tissue-derived progenitor cells based on RAD16-I self-assembling peptide. Tissue Eng Part C Methods 2016; 22: 113-124.

[16] Reecha-Sancho L, Moutos FT, Abella J, Guilak F and Semino CE. Dedifferentiated human articular chondrocytes redifferentiate to a cartilage-like tissue phenotype in a poly(ε-caprolactone)/self-assembling peptide composite scaffold. Materials (Basel) 2016; 9: 472.

[17] Wang X, Ma S, Meng N, Yao N, Zhang K, Li Q, Zhang Y, Xing Q, Han K, Song J, Yang B and Guan F. Resveratrol exerts dosage-dependent effects on the self-renewal and neural differentiation of hUC-MSCs. Mol Cells 2016; 39: 418-425.

[18] Ma S, Liang S, Jiao H, Chi L, Shi X, Tian Y, Yang B and Guan F. Human umbilical cord mesenchymal stem cells inhibit C6 glioma growth via secretion of dickkopf-1 (DKK1). Mol Cell Biochem 2014; 385: 277-286.

[19] Kang J, Zhang Z, Wang J, Wang G, Yan Y, Qian H, Zhang X, Xu W and Mao F. hucMSCs attenuate IBD through releasing miR-148b-5p to inhibit the expression of 15-lox-1 in macrophages. Mediators Inflamm 2019; 2019: 6953063.

[20] Alemany-Ribes M, Garcia-Diaz M, Busom M, Nonell S and Semino CE. Toward 3D cellular model for studying in vitro the outcome of photodynamic treatments: accounting for the effects of tissue complexity. Tissue Eng Part A 2013; 19: 1665-1674.

[21] Livak KJ and Schmittgen TD. Analysis of relative gene expression data using real-time quantitative PCR and the $2^{-\Delta\Delta ct}$ method. Methods 2001; 25: 402-408.

[22] Wan S, Borland S, Richardson SM, Merry CLR, Saiani A and Gough JE. Self-assembling peptide hydrogel for intervertebral disc tissue engineering. Acta Biomater 2016; 46: 29-40.

[23] Soler-Botija C, Bago JR, Llucia-Valldeperas A, Valles-Lluch A, Castells-Sala C, Martinez-Ramos C, Fernandez-Muinos T, Chachques JC, Pradas MM, Semino CE and Bayes-Genis A. Engineered 3D bioimplants using elastomeric scaffold, self-assembling peptide hydrogel, and adipose tissue-derived progenitor cells for cardiac regeneration. Am J Transl Res 2014; 6: 291-301.

[24] Kim JE, Kim SH and Jung Y. In situ chondrogenic differentiation of bone marrow stromal cells in bioactive self-assembled peptide gels. J Biosci Bioeng 2015; 120: 91-98.

[25] Gottlieb D, Morin SA, Jin S and Raines RT. Self-assembled collagen-like peptide fibers as templates for metallic nanowires. J Mater Chem 2008; 18: 3865.

[26] Maranda EL, Rodriguez-Menocal L and Badiavas EV. Role of mesenchymal stem cells in dermal repair in burns and diabetic wounds. Curr Stem Cell Res Ther 2017; 12: 61-70.

[27] Yin S, Ji C, Wu P, Jin C and Qian H. Human umbilical cord mesenchymal stem cells and exosomes: bioactive ways of tissue injury repair. Am J Transl Res 2019; 11: 1230-1240.

[28] Danielson JJ, Perez N, Romano JD and Coppens I. Modelling toxoplasma gondii infection in a 3D cell culture system in vitro: comparison with infection in 2D cell monolayers. PLoS One 2018; 13: e0208558.

[29] Shi W, Huang CJ, Xu XD, Jin GH, Huang RQ, Huang JF, Chen YN, Ju SQ, Wang Y, Shi YW, Qin JB, Zhang YQ, Liu QQ, Wang XB, Zhang XH and Chen J. Transplantation of RADA16-BDNF peptide scaffold with human umbilical cord mesenchymal stem cells forced with CXCR4 and activated astrocytes for repair of traumatic brain injury. Acta Biomater 2016; 45: 247-261.

[30] Zhang L, Li Y, Guan CY, Tian S, Lv XD, Li JH, Ma X and Xia HF. Therapeutic effect of human umbilical cord-derived mesenchymal stem cells on injured rat endometrium during its chronic phase. Stem Cell Res Ther 2018; 9: 36.

[31] Shi Q, Gao J, Jiang Y, Sun B, Lu W, Su M, Xu Y, Yang X and Zhang Y. Differentiation of human umbilical cord Wharton's jelly-derived mesenchymal stem cells into endometrial cells. Stem Cell Res Ther 2017; 8: 246.

[32] Lyons FG and Mattei TA. Sources, identification and clinical implications of heterogeneity in human umbilical cord stem cells. Adv Exp Med Biol 2019; 1169: 243-256.

[33] Trusler O, Huang Z, Goodwin J and Laslett AL. Cell surface markers for the identification and study of human naive pluripotent stem cells. Stem Cell Res 2018; 26: 36-43.

[34] Skurikhin EG, Pakhomova AV, Ermakova NN, Pershina OV, Pan ES, Ermolaeva LA, Kudryashova AI, Krupin VA, Rybalkina OY and Dygai AM. Response of stem and progenitor cells to testicular ischemia. Bull Exp Biol Med 2016; 161: 523-528.

[35] Tao R, Sun TJ, Han YQ, Xu Q, Liu J and Han YF. Epimorphin-induced differentiation of human umbilical cord mesenchymal stem cells into sweat gland cells. Eur Rev Med Pharmacol Sci 2014; 18: 1404-1410.

[36] Zhang L, Tan X, Dong C, Zou L, Zhao H, Zhang X, Tian M and Jin G. In vitro differentiation of human umbilical cord mesenchymal stem cells (hUCMSCs), derived from Wharton's jelly, into choline acetyltransferase (ChAT)-positive cells. Int J Dev Neurosci 2012; 30: 471-477.

[37] Zhang D, Liu D, Zhang J, Fong C and Yang M. Gold nanoparticles stimulate differentiaiton and mineralization of primary osteoblasts through the ERK/MAPK signaling pathway. Mater Sci Eng C Mater Biol Appl 2014; 42: 70-77.

[38] Black KA, Lin BF, Wonder EA, Desai SS, Chung EJ, Ulery BD, Katari RS and Tirrell MV. Biocompatibility and characterization of a peptide amphiphile hydrogel for applications in peripheral nerve regeneration. Tissue Eng Part A 2015; 21: 1333-1342.